DOI: 10.3901/CJME.2011.04.***, available online at www.cjmenet.com; www.cjmenet.com.cn

Numerical Analysis of Nozzle Clearance's Effect on Turbine Performance

HU Liangjun[1]*, YANG Ce[1], SUN Harold[2], ZHANG Jizhong[3], and LAI MingChia[4]

1 School of Mechanical Engineering, Beijing Institute of Technology, Beijing 100081, China
2 Ford Motor Company, Michigan, 48124 USA
3 National Key Laboratory of Diesel Engine Turbocharging Technology, Datong, Shanxi 037036, China
4 Wayne State University, Michigan, 48122 USA

Received September 22, 2010; revised March 17, 2011; accepted March 21 2011; published electronically March 23, 2011

Abstract: Variable nozzle turbine (VNT) has become a popular variable geometry turbine (VGT) technology for the diesel engine application. Nozzle clearance, which can't be avoided on the hub and shroud side of the VNT turbine due to the pivoting stators, can lead to turbine performance deterioration. However, its mechanism is still not clear. In this paper, numerical investigation, which is validated by experiment, is carried out to study the mechanism of the nozzle clearance's effect on the turbine performance. Firstly, performance of the mixed flow turbine with fixed nozzle clearanceis tested on flow bench. Performance of the tested turbine with the same nozzle clearance is numerically simulated. The numerical result agrees well with the test data, which proves correct of the numerical method. Then the turbine performance with different nozzle clearances is numerically analyzed. The research showed that with nozzle clearance, flow loss in the nozzle increases at first and it reaches the maximum value when the clearance ratio is 5%. Flow at the exit of the nozzle becomes less uniform with nozzle clearance. The negative incidence angle of the rotor also increases with nozzle clearance and leads to more incidence angle loss in the rotor. The low energy fluid formed in the nozzle due to the nozzle clearance migrates from hub to shroud side in the rotor, which is another main reason for the rotor's performance degradation. The present research exposed the mechanism of the dramatically decrease of the turbine performance with nozzle clearance: (a) The loss associated with the nozzle leakage increases with the nozzle clearance; (b) The flow loss grows up quickly in the rotor due to the incidence angle loss and migration of the low energy fluid from hub to shroud side.

Key words: nozzle clearance, variable nozzle turbine (VNT), mixed flow turbine

1 Introduction

Turbocharger has been widely applied on diesel engine to improve the engine's power, efficiency, and exhaust emissions. The installation of turbocharger for a diesel engine is now indispensable. In the last decade, variable geometry turbines (VGT) have received a lot of attention and been widely applied in diesel engines. VGT could improve the diesel engines' fuel economy and emissions [1–3]. Many researches have been carried out on the variable geometry turbocharger, including the development of variable nozzle geometry, variable inlet vane, twin scroll switching, et al[4–7]. Nowadays, the dominant VGT technology for diesel application is the variable nozzle turbine (VNT)[8, 9]. It uses pivoting vanes to change the speed and angle of the exhaust gas when it enters the turbine rotor. VNT turbine's peak efficiency is lower than that of the turbine without variable geometry due to the clearance both on the hub and shroud side of the variable nozzle. SPENCE, et al[10], investigated the nozzle's flow field variation due to the nozzle clearance. His research showed that the nozzle clearance leakage flow changes considerable at different vane positions and flow incidence at vane inlet has a significant effect on turbine performance. TAMAKI, et al[11], studied the nozzle clearance's effect on radial turbine's performance. His research found that the nozzle clearance leakage flow increases when the nozzle's opening decreases. Some predicting methods for VNT with nozzle clearance have also been reported[12–14]. However, most of the researches were based on the overall performance without the mechanism analyses of nozzle clearance's effect on turbine performance and no research have been carried out on how the nozzle clearance affecting the rotor's performance.

Computation fluid dynamics (CFD) have become an important tool in the design and analysis of turbomachinery. CFD is able to predict the performance and internal flow field of the turbine very well[15, 16]. Due to the small size and high speed of the turbocharger for automotive engine, direct measurement of the internal flow field is quite difficult. As a result, CFD simulation is employed to investigate the nozzle clearance's effect on the turbine performance.

*Corresponding author Email: lhu0808@gmail.com
This project is supported by Advanced Boost System Development for Diesel HCCI Application of DOE(Grant No. DE-FC26-07-NT43280)

In present research, firstly overall performance of the designed mixed flow turbine was simulated at full opening position of the nozzle vane. Numerical simulation was also validated by test data. Then the performances of the turbine with different nozzle clearance were analyzed and the losses of the nozzle were calculated. The performance deterioration of the rotor due to the nozzle clearance was also investigated. Finally, detailed internal flow field with and without nozzle clearance were compared to study how the nozzle clearance affects the rotor's performance.

2 Test and Numerical Model of the Turbine

To improve performance of the turbine at low velocity ratio area, a mixed flow turbine was designed and manufactured to adapt with the existing VNT system. There are 9 nozzle vanes and 13 rotor blades. Preliminary CFD showed that there was only a little efficiency penalty when the mixed flow turbine matches with the straight vane. Besides that, redesign of the nozzle and the actuation system requires much more cost. As a result, a mixed flow turbine was designed without modification of the straight nozzle. Fig. 1 shows the meridional view of the turbine with nozzle clearance on the hub and shroud side. Fig. 2 is the 3D model of the turbine. Performance of the turbine was tested on flow bench with an even clearance ratio c/b=2% (c is the nozzle clearance and b is the width of the nozzle) on the hub and shroud side separately. High pressure air provided by air supply was heated when it flowed through the electric heater. Then the air with high pressure and temperature was used to drive the turbine. At the turbine inlet, total pressure and temperature were measured. At turbine outlet, static pressure and total temperature were measured. All the flow parameters were measured with three probes and the averaged value was used for the calculation of the turbine's performance. The uncertainty of the stage pressure ratio and efficiency was within 1%. Test and simulation was carried out at full opening position of the nozzle.

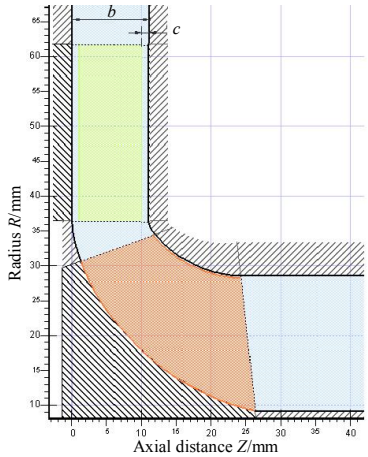

Fig. 1 Meridional view of the turbine

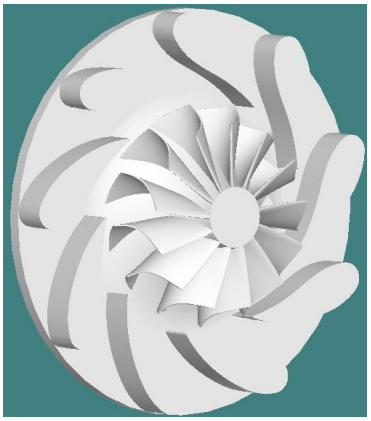

Fig. 2 3D model of the turbine

Commercial code EURANUS, integrated in Fine/Turbo interface, was used in the numerical simulation. It solves the time dependent Reynolds averaged N-S equations. The equations were discredited using a central difference scheme and a steady state flow solution was achieved upon the convergence of a 4 stage explicit Runge-Kutta integration scheme. To speed up the convergence, a full multi-grid technique was applied. The one-equation turbulence model, Spalart-Allmaras model, was used in the present simulation.

In present research, single passage of the nozzle and rotor were modeled and mixing plane was used between the rotor and stator interface. At nozzle inlet, total temperature and pressure were applied. Nozzle inlet flow direction was calculated according to the geometry of volute and applied at computation domain inlet. At rotor outlet, static pressure was assumed to be uniform along the tangential direction and the value at specific radius was applied. The static pressure distribution along the radial direction was given by the following equation:

$$\frac{\partial p}{\partial r} = \rho \cdot \frac{v_\theta^2}{r}.$$

Adiabatic and non-slip wall boundary conditions were imposed.

Multi-block structure mesh of the rotor and nozzle was generated by IGG/AutoGrid automatically. To capture the geometry of the impeller and improve the mesh quality, O mesh was used around the nozzle and rotor blade surface blocks and H mesh was used in the other blocks. Grid clustering was applied around all the wall surfaces to calculate the boundary layer and an averaged y^+ of 3 was achieved.

Fig. 3 Mesh distribution of the nozzle

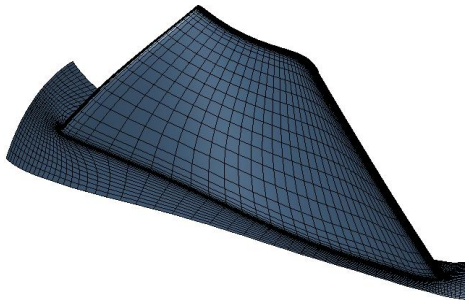

Fig. 4 Mesh distribution of the rotor

By varying the node distribution inside the nozzle clearance, the O block around the blade surface, along the stream-wise and span-wise directions, three different meshes were generated for the nozzle and rotor. Then simulation was carried out at peak efficiency point of the chosen turbo speed. The result was shown in table 1. With the three different meshes, the predicted performance of the turbine was less than 0.1%. With increased mesh density, the predicted performance would be more accurate but at the expense of more computer resources and simulation time. In present research, the second mesh was used to simulate the overall performance of the turbine and to study the nozzle clearance's effect on the turbine performance.

Table 1 Grid sensitivity study of the turbine

Mesh size	Mass flow M/(kg·s^{-1})	Pressure ratio Pr	Efficiency η
463 172	0.128 7	1.253 6	0.762 3
626 292	0.128 9	1.253 6	0.764 5
1 436 100	0.129 1	1.253 7	0.764 4

3 Validation of the CFD

The overall performances of the turbine from low to high velocity ratios were simulated and compared with the test data. The result is shown in Fig. 5. Due to the limitation of the power absorbed by the compressor, test data was only available in a much narrower range compared to the CFD result. Within the test data's range, the predicted pressure ratio of the turbine was about 2% higher than the test result. This may be mainly due to the model difference in the simulation and test: volute wasn't modeled in the simulation thus the flow loss of the volute wasn't included; at the same mass flow rate, the pressure ratio of the turbine calculated without volute would be higher than the one with volute. Fig. 5(b) shows the variation of the efficiency with velocity ratio. The predicted efficiency tendency of the turbine agrees well with the test data. As no volute loss was calculated, the predicted efficiency is about 2–3% higher than test data. Despite of this discrepancy, it can be seen that CFD is able to predict the performance of the turbine very well and the CFD simulation could be used to analyze the turbine performance.

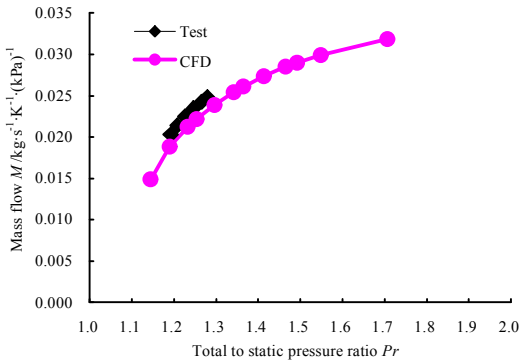

(a) Mass flow of the turbine

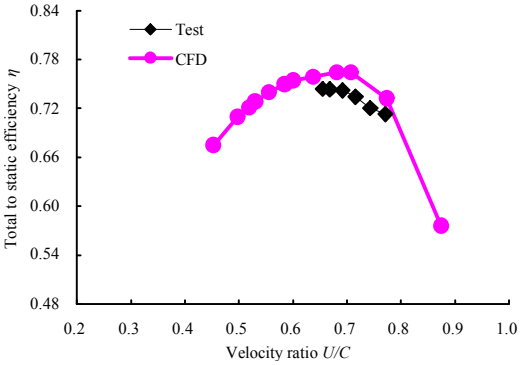

(b) Efficiency of the turbine

Fig. 5 Comparison of turbine performance between CFD and test data

4 Analysis of different nozzle clearances' effect on the turbine performance

To study the nozzle clearance's effect on the turbine performance, simulation was carried out with different and without nozzle clearances. In present research, fixed turbine housing, i.e. fixed turbine shroud and hub line, was assumed. By changing the height of the nozzle vane, the nozzle clearance could be changed. Even clearance on the hub and shroud side was applied. Five different nozzle clearances were modeled here: c/b=2%, 3%, 4%, 5% and 6%. Fig. 6 shows the performance comparison with and without nozzle clearance. It can be seen that efficiency of the turbine drops quickly with increase of the nozzle clearance. Compared to the one without nozzle clearance, the peak efficiency of the turbine with 2% of nozzle clearance has dropped about 3% while at higher U/C area the efficiency of the turbine drops less. With 1% increase in nozzle clearance, the efficiency of the turbine drops about 2.5%. Obviously, the turbine efficiency is quite sensitive to the nozzle clearance. Fig. 6(b) shows the flow rate of the turbine with different nozzle clearance. With increased nozzle clearance, the flow passage of the nozzle would be increased and the same as the flow capacity of the turbine.

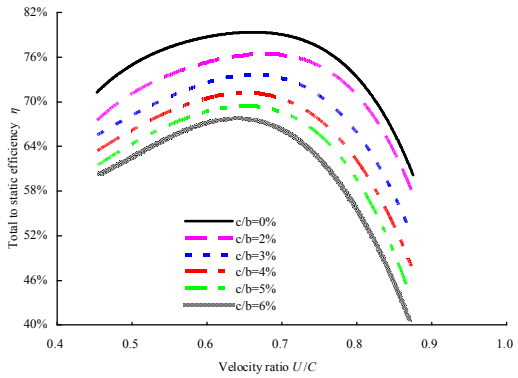

(a) Efficiency of the turbine

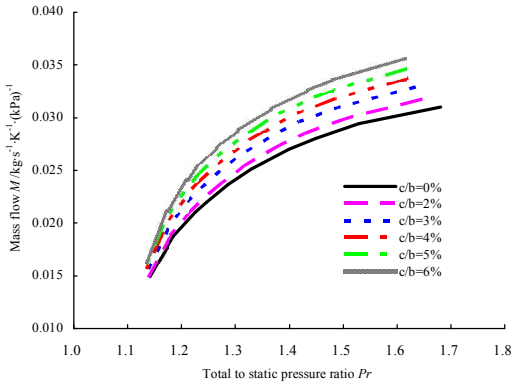

(b) Mass flow of the turbine

Fig. 6 Comparison of turbine's performance with different and without nozzle clearance

To investigate the loss of the nozzle and rotor due to the nozzle clearance, the peak efficiency point, U/C=0.68, was chosen to analyze the performance of the rotor and nozzle. Fig. 7 shows the efficiency decrement of the nozzle with increase of the nozzle clearance. The efficiency decrement of the nozzle was calculated according to the following equations:

$$\omega = \eta_{\text{rotor}} - \eta_{\text{stage}}$$

where ω is the efficiency decrement of the nozzle, η_{rotor} and η_{stage} are the total to static efficiency of the rotor and stage separately. It can be seen that without nozzle clearance, there is only about 2% in loss caused by the nozzle. With increase of the nozzle clearance, the efficiency decrement of the nozzle grows up gradually. When the clearance ratio is up to 5%, the efficiency decrement of the nozzle almost keeps the same. The maximum efficiency decrement of the nozzle is about 7%.

Fig. 8 shows the variation of the rotor's efficiency with nozzle clearance. It can be seen that nozzle clearance also leads to degradation of the rotor performance. Compared to the case without nozzle clearance, with 2% of nozzle clearance, the peak efficiency of the rotor deteriorates about 0.5%; with 3% of nozzle clearance, the rotor's efficiency drops about 2%, and it increases to 3% when the nozzle clearance is increased to 4%. The efficiency of the rotor deteriorates quickly if the nozzle clearance is further increased. It can be seen that with increase of the nozzle clearance, the deterioration of the rotor plays a more important role in the degradation of the stage efficiency.

From the above analysis, it is clear that the nozzle clearance not only leads to extra loss of the leakage flow inside the nozzle, it also leads to performance deterioration of the rotor. As a result, turbine's efficiency is very sensitive to the nozzle clearance.

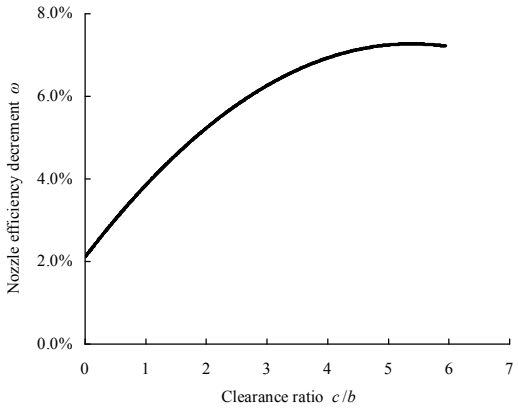

Fig. 7 Nozzle efficiency decrement

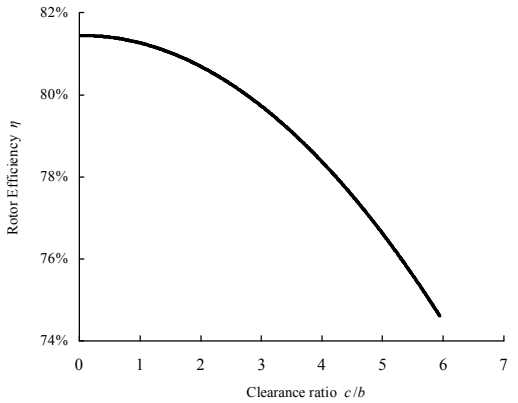

Fig. 8 Variation of rotor peak efficiency with nozzle clearance

5 Detailed flow field analysis

Investigation of the internal flow field helps to understand the loss inside the nozzle and rotor. The two cases, with 4% of nozzle clearance and without nozzle clearance, were chosen to compare the change in flow field due to nozzle clearance. All of the following flow field comparison was carried out at U/C=0.68 at which the turbine stage reaches the peak efficiency.

Fig. 9 shows the entropy distribution on 90% spanwise of the nozzle, which is close to the shroud side. Without nozzle clearance, there is high entropy on the suction side of the nozzle. It is due to that the air speeds up in the nozzle and the velocity on the suction side is larger than that the pressure side, as a result, there is more friction loss on the suction side. There is also a high entropy area in the trailing edge of the nozzle, which is mainly caused by the blade wake flow. Streamline in Fig. 10(a) shows that air is able to flow through the nozzle passage smoothly without

separation flow. At this condition, the main loss inside the nozzle is the friction and the wake flow loss. With nozzle clearance, the friction loss on the pressure side of the nozzle is almost the same as the one without nozzle clearance. The wake flow can also be observed. However, there is an area with high entropy right after the throat of the flow passage, which is very close to the suction side. Streamline in Fig. 10(b) shows that this is mainly caused by the leakage flow. Driven by the pressure gradient between the pressure and suction side of the nozzle, the air flows from the pressure side to the suction side of the nozzle through nozzle clearance, as illustrated by the streamline. When mixing with the main flow, it leads to extra loss inside the flow passage. The leakage flow has the tendency to roll up and then strong leakage vortex is formed near the suction side. The peak entropy area shows the path of the leakage vortex. The more leakage flow, the more loss is generated. On the hub side, the high entropy area resides almost the same location on the shroud side. But in the center of the leakage vortex, the entropy has been increased a little, indicating that the loss due to leakage has been increased on the hub side. This may be due to the different turning angle of the main flow on the hub and shroud side (viewing meridionally): on the hub side, there is less turning angle of the flow and more fluid could flow through the passage; as a result, more leakage flow and more leakage losses are generated on the hub side.

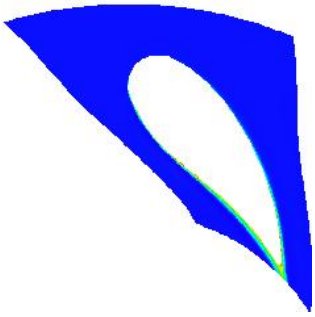

(a) Without nozzle clearance

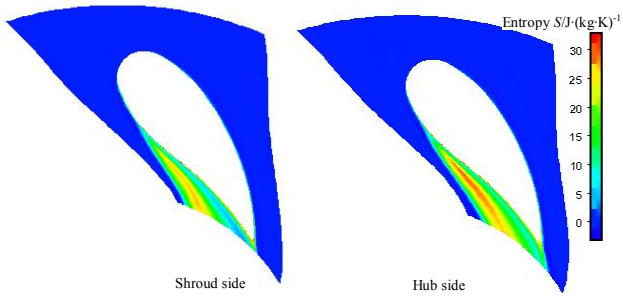

(b) With nozzle clearance

Fig. 9 Entropy distribution of the nozzle

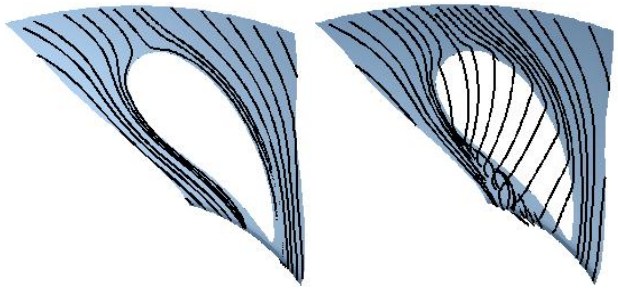

(a) Without nozzle clearance (b) With nozzle clearance

Fig. 10 Streamline of the nozzle

Fig. 11 shows the total pressure distribution at the trailing edge of the nozzle with and without nozzle clearance. Without nozzle clearance, there is a strip with low pressure from hub to shroud side. It is caused by the wake flow of the nozzle blade. On the hub side, the low pressure layer is thicker than that on the shroud side. This is mainly due to the fact that there is more flow through the passage near the hub side than the shroud side, thus there is more boundary layer loss on the hub side. With nozzle clearance, the wake flow after the blade and boundary layer on the end wall still could be observed. But there are two separate areas with low pressure near the hub and shroud. This is mainly induced by the nozzle clearance leakage flow. On the hub side, there is more total pressure loss compared to the shroud side, similar to the entropy distribution shown in Fig. 9. With nozzle clearance, the flow distribution at the exit of the nozzle is less uniform and the effect on the performance of the rotor, which is located in the downstream of the nozzle, needs to be investigated.

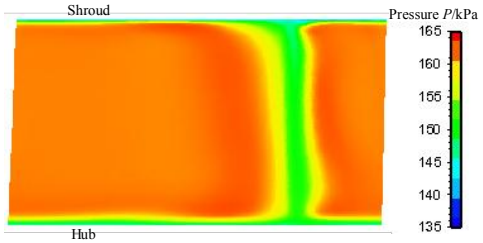

(a) Without nozzle clearance

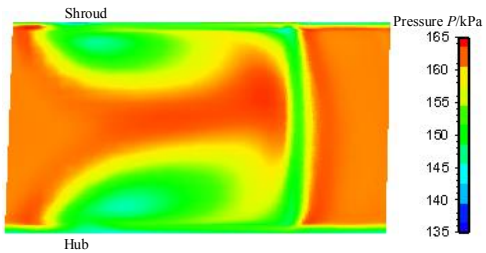

(b) With nozzle clearance

Fig. 11 Total pressure distribution on the trailing edge of the nozzle

Fig. 12 shows the relative flow angle at the rotor inlet. Without nozzle clearance, the flow angle near the shroud

side is slightly lower than the hub side. But the flow angle variation is very small and its distribution is relatively uniform in most of the area. The averaged flow angle is -15.5° . With nozzle clearance, the relative flow angle near the hub and shroud side has been increased significantly and the maximum flow angle is located near the mid span of the rotor. This change of the relative flow angle could be explained as follows: With nozzle clearance, the fluid flows from the pressure side to the suction side of the nozzle and the tangential velocity (counter of the turbine's rotation direction) at the nozzle's exit is increased. In other words, the inlet tangential velocity of the rotor has been increased along the opposite rotation direction of the rotor. As a result, the relative flow angle of the rotor decreases on the hub and shroud side. Then the incidence angle of the rotor has been increased near the hub and shroud side. With nozzle clearance, the inlet condition of the rotor has been changed and the performance of the rotor is affected consequently.

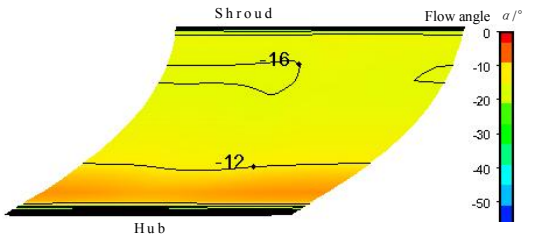

(a) Without nozzle clearance

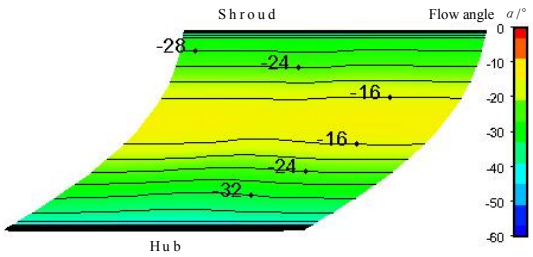

(b) With nozzle clearance

Fig. 12 Relative flow angle distribution of rotor inlet

Fig. 13 presents the limiting streamlines on the suction surface with and without nozzle clearance. Without nozzle clearance, there is neither separation line nor attachment line at the impeller inlet, indicating that the flow in this area is very smooth. There is an attachment line near the shroud of the impeller starting just after the leading edge to about 50% chord. The development of tip leakage vortex corresponds to the existence of the attachment line along the blade tip. A separation line can be seen starting from about 40% chord near hub to 70% chord near shroud. This could be explained as follows: The flow has the tendency to turn from radial direction to axial direction inside the turbine; at the same time, due to the centrifugal force effect, the low energy fluid near hub flows toward the tip; those two effects combined together leads to formation of the separation line as shown in Fig. 13(a). With nozzle clearance, the attachment line near the shroud due to the tip leakage vortex is similar to the one without nozzle clearance. But at impeller inlet near hub, the fluid starts to flow towards the blade tip, which is different from the case without nozzle clearance. Due to the nozzle clearance, the fluid at impeller inlet near hub also has relative slow radial velocity and it couldn't overcome the centrifugal force. As a result, the low energy fluid begins to migrate from hub towards shroud side at impeller inlet. The result is that the low energy fluid occupies more flow passage and more loss is generated compared to the one without nozzle clearance.

Fig. 14 shows the limiting streamline on the pressure surface with and without nozzle clearance. Without nozzle clearance, there is an attachment line starting from about 35% spanwise at impeller inlet. This is mainly caused by the centrifugal force and blade curvature. Above the attachment line, the fluid has the tendency to move towards the shroud. There is also a separation line parallel to the leading edge of the impeller from about 70% spanwise to shroud side, which is mainly due to the negative incidence angle. With the thick blunt trailing edge and the wake flow, separation and attachment line could be observed near the trailing edge. With nozzle clearance, the separation line which is parallel to the leading edge of the rotor close to the shroud side still exists, and on the hub side there is also a separation line due to the increased negative incidence angle. From the impeller leading edge to about 20% chord, there is reverse flow from hub to shroud side. Starting from about 20% chord, there is an attachment line along which the fluid attaches to the blade surface.

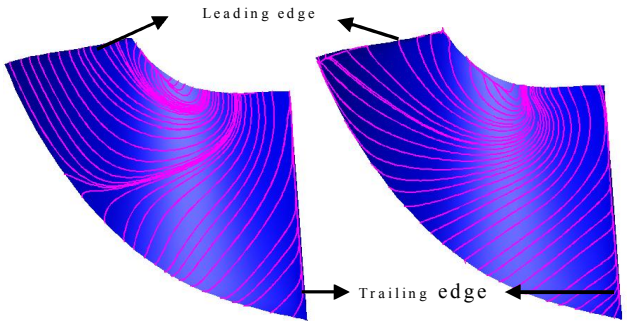

(a) Without nozzle clearance (b) With nozzle clearance

Fig. 13 Limiting streamline on suction surface

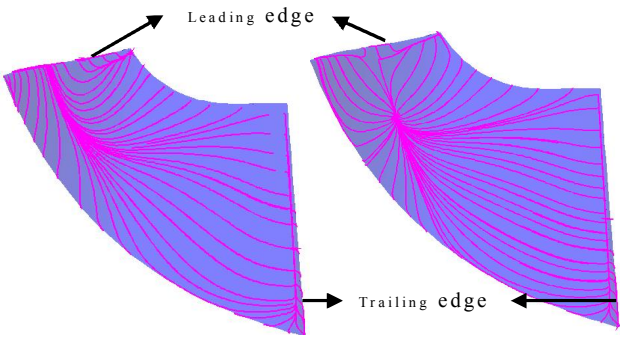

(a) Without nozzle clearance (b) With nozzle clearance

Fig. 14 Limiting streamline on pressure surface

From the above analysis, it can be seen that with nozzle clearance, there is more low energy fluid migration from hub to shroud side due to the centrifugal force. Besides that, with increased negative incidence angle, there is flow separation on the pressure side, which leads to more loss inside the rotor passage.

Fig. 15 shows the entropy distribution of the rotor at 90% spanwise near shroud. Without nozzle clearance, there is a high entropy area on the suction side starting from the leading edge of the rotor and it grows up gradually along the flow direction. It's mainly caused by the secondary flow and migration of the low energy fluid from hub to shroud side. The low energy fluid also interacts with the rotor tip leakage near the shroud side. With nozzle clearance, the high entropy area on the suction side is similar to the one without nozzle clearance except that starting from about 30% chord length the peak entropy has been increased. Compared with the limiting streamline in Fig. 13 and 14, it can be seen that increase of the entropy is mainly due to the increase of the low energy fluid migration from hub to shroud side.

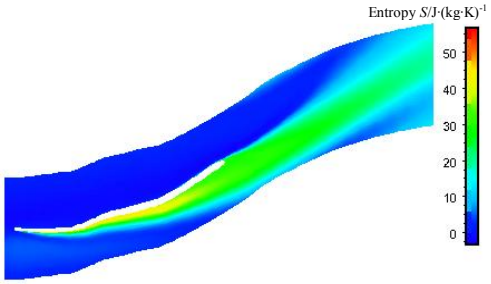

(a) Without nozzle clearance

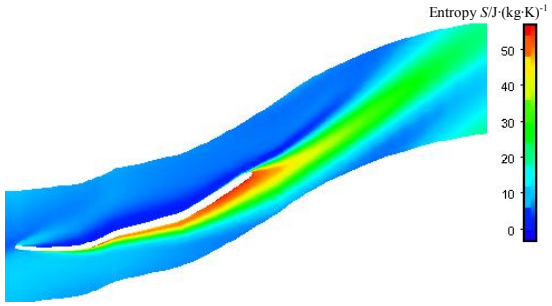

(b) With nozzle clearance

Fig. 15 Entropy distribution on 90% spanwise

Fig. 16 shows the entropy comparison on 10% spanwise of the rotor with and without nozzle clearance. It can be seen that without nozzle clearance, there is some high entropy area on the suction side from 20% to 60% chord length. With nozzle clearance, the high entropy area on the suction side has been increased a lot, which is also the effect of the low energy fluid migration. On the pressure side near the leading edge of the rotor, there is an area with high entropy which is mainly caused by the negative incidence angle.

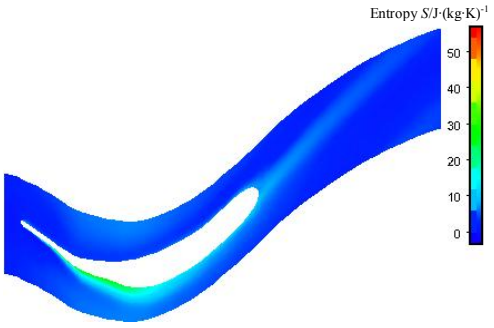

(a) Without nozzle clearance

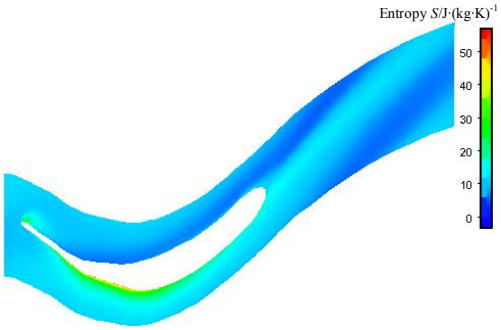

(b) With nozzle clearance

Fig. 16 Entropy distribution on 10% spanwise

With nozzle clearance, the entropy distribution shows that the flow loss in the rotor has been increased both on the hub and shroud side. The efficiency of the rotor with nozzle clearance has deteriorated substantially.

6 Conclusions

(1) The turbine stage performance is very sensitive to the nozzle clearance; the stage efficiency deteriorates gradually with increase of the nozzle clearance;

(2) With increase of nozzle clearance, the efficiency decrement of the nozzle also increases at first due to the leakage both on the hub and shroud side; when the clearance ratio is up to 5%, the efficiency decrement of nozzle reaches the maximum value;

(3) With nozzle clearance, the exit flow condition of the nozzle is less uniform and the tangential velocity (counter to the rotation direction) is increased. As a result, the negative incidence angle at the rotor inlet is increased and the same as the incidence angle loss of the rotor;

(4) The low energy fluid formed by the leakage inside the nozzle has the tendency to migrate from hub to shroud side in the rotor passage due to the centrifugal force. It leads to increase of the flow loss and is another main reason for the rotor's performance degradation.

References

[1] WATSON N, JANOTA M S. *Turbocharging the Internal Combustion Engine*[M]. New York: Jonh Wiley & Sons Inc, 1982.

[2] BAINES N C. Radial and mixed flow turbines options for high boost turbocharger[C]//*7th Int. Conference on Turbocharger and Turbocharing in Savoy Palace*, London, UK, May 14−15, 2002:

35−44.
[3] MOODY J F. Variable geometry turbocharging with electronic control[C]. *SAE Paper*, 860107.
[4] ROGO C, HAJEK T, RELKE R. Aerodynamic effects of moveable sidewall nozzle geometry and rotor exit restriction on the performance of a radial turbine[C]. *SAE Paper*, 831517.
[5] ARNOLD S. Schwitzer variable geometry turbo and microprocessor control design and evaluation[C]. *SAE Paper*, 870296.
[6] FRANKLIN P C. Performance development of the holset variable geometry turbocharger[C]. *SAE Paper*, 890646.
[7] KAWAGUCHI J, ADACHI K, KONO S T. Development of VFT (Variable Flow Turbocharger)[C]. *SAE Paper*, 1999-01-1242.
[8] ZHANG J Z, ZHUGE W L, HU L F. Design of turbocharger variable nozzle[C]. *ASME Paper*, GT2007-27562.
[9] ARNOLD S. Advanced variable geometry turbocharger for diesel engine applications[C]. *SAE Paper*, 2002-01-0161.
[10] SPENCE S W, NEILL J W, CUNNINGHAM G. An investigation of the flow field through a variable geometry turbine stator with vane endwall clearance[J]. *Proceedings of the Institution of Mechanical Engineers Part A: Journal of Power and Energy*, 2006, 220, 899−910.
[11] TAMAKI H, GOTO S, UNNO M. The effect of clearance flow of variable nozzle on radial turbine performance[C]. *ASME Paper*, GT2008-50461.
[12] MATSUNMOTO K, JINNAI Y. Development of variable geometry turbocharger for diesel passenger car[C]//*The 6th International Conference on Turbocharging and Air Management System*, London, UK, Novermber 3−5, 1998: 329−346.
[13] OKAZAKI Y, MATSUDAIRA N. A case of variable geometry turbocharger development[C]//*The Third International Conference on Turbocharging and Turbochargers*, Birdcage Walk, London, UK, May 6-8, 1986: 191−195.
[14] MEITNER P L, GLASSMAN A J. Loss model for off-design performance analysis of radial turbines with pivoting-vane variable-area[C]. *SAE Papers*, 801135.
[15] SIMPSON A T, SPENCE S W, WATTERSON J K. A comparison of the flow structures and losses within vaned and vanlelss stators for radial turbines[J]. *Transactions of the ASME, Journal of turbomachinery*, 2007, 129(1): 53−61.
[16] SIEROS G, KEFALAKIS M, PAPAILIOU D K. Improved turbine performance by use of CFD[C]. *ASME Paper*, GT2004−53737.

Biographical notes

HU Liangjun, born in 1982, is currently a PhD candidate at *School of Mechanical Engineering, Beijing Institute of Technology, China*. His main research field is turbomachinery aerodynamics.
E-mail: lhu0808@gmail.com.

YANG Ce, PhD, born in 1964, is currently a professor at *Beijing Institute of Technology, China*. He received his PhD degree at engineering from *Tsinghua University, China*, in 1998. He has published a book and more than 50 papers. His main research field is turbomachinery aerodynamics.
Tel: +86-10-68911373; E-mail: yangce@bit.edu.cn

SUN Harold, PhD, born in 1960, is currently a technical expert at *Research and Innovation Center, Ford Motor Company, Michigan, USA*. Over more than 20 years, his careers include engine combustion research, diesel engine development and boost system research.
E-mail: hsun3@ford.com.

ZHANG Jizhong, born in 1970, is currently a research fellow in *National Key Laboratory of Diesel Engine Turbocharging Technology, China*. His research interest is in the field of the turbocharging technology for diesel engine.
E-mail: jizhong.zhang@gmail.com.

Lai Mingchia, PhD, born in 1957, is currently a professor of mechanical engineering at *Wayne State University, Detroit, Michigan, USA*. His primary research skills and interests are in the fields of thermal-fluid engineering, IC engines, gas turbine combustion, and energy conversion.
E-mail: lai@eng.wayne.edu.